

# EFFECT OF ELECTRODE GEOMETRY ON RESISTANCE SPOT WELDING OF AHSS

Kevin R. Chan, Nigel Scotchmer  
Huys Welding Strategies Ltd., 175 Toryork Road Unit #35, Weston, Ontario,  
Canada

John C. Bohr  
General Motors - North America, Controls, Conveyors, Robotics and Welding,  
30300 Mound Road, Warren, MI 48090-9015

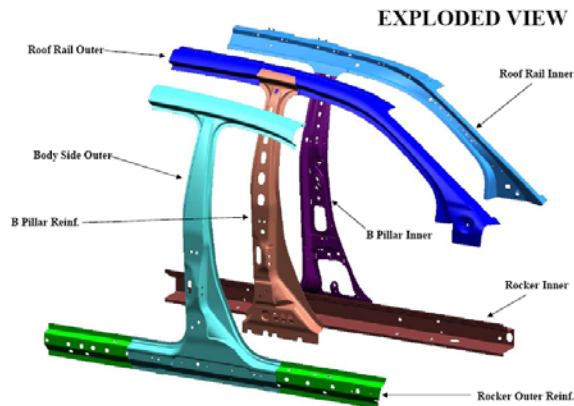
Ibraheem Khan, Michael L. Kuntz, Y. Norman Zhou  
Centre for Advanced Materials Joining, University of Waterloo,  
200 University Ave. W, Waterloo, ON N2L 3G1

## ABSTRACT

The implementation of advanced high strength steels (AHSS) into the automotive industry offers distinct advantages relative to achieving light weighting goals and improved structural performance. The challenge for the automotive industry is a need to develop the processes and know-how to implement these new materials into their product economically. Currently the primary method used to develop spot welding practices for new material involves both extensive and costly laboratory trial and error experimentation.

The finite element method was used as a low cost alternative for the fundamental development of joining practices for AHSS. Specifically, the effect of electrode geometry on nugget formation in typical AHSS resistance spot weld applications was investigated.

The weld joint chosen for the study was based on an Auto-Steel Partnership (A/SP) state-of-the-art B-Pillar to rocker joint using 1.6 mm GI DP780 to 1.6 mm GI DP780 (B pillar reinforcement to rocker outer reinforcement). The effect of electrode cap geometry was modeled using SORPAS® resistance spot welding FEA software. The results were verified experimentally at the University of Waterloo Centre for Advanced Materials Joining.



Courtesy A/SP Joining Technologies 2006

Four electrode geometries were compared, including standard domed-flat (B-nose with 4.8 mm flat), truncated (E-nose 45° with 6 mm flat), B-nose (ISO F-style) with 6 mm flat, and a new parabolic shaped electrode (ParaCap™, 6 mm flat). All electrodes were copper chromium zirconium alloys.

Construction of weldability windows in terms of weld current was facilitated by simulations and showed the differences between the electrode geometries. It was found that the shape of the electrodes had an influence on the development and final shape of the weld nugget. The usable range of current between minimum weld size and nominal weld size was found to be largest for the ParaCap™ electrode. Weld schedules and nugget shapes were compared to lab testing on coupons and were found to exhibit similar trends for schedules and nugget sizes.

Finite modeling of the resistance spot welding process along with lab testing was able to illustrate the behaviour of different electrode geometries and proved to be a useful tool in understanding the effect of electrode cap geometry on the weldability of AHSS. The information obtained through simulations can be of great assistance in the implementation of these new steels in the automotive industry and useful as a cost saving tool.

## INTRODUCTION

The parallel drive for better crash performance and improved fuel economy have led the automotive industry to adopt stronger steels, such as AHSS, that can reduce weight by providing the same tensile strength of thicker material. However, the implementation of AHSS into the automotive industry has thus far encountered difficulty due, in part, to welding issues. These issues revolve around different characteristics of strength and ductility that vary from the more common steels [Ref.1]. Automotive manufacturers need to know whether these new materials can be integrated into existing product designs and manufacturing processes with minimal or no change to existing plant floor production equipment. The weldability evaluation of this material must take into account the various manufacturing processes already in existence, AC versus DC, traditional schedules versus pulsation, use of different weld forces, and type and geometry of electrode. Without being able to understand and optimize how to join these next generation materials to themselves and other materials, their use and benefits become restricted.

In current automotive practice there is a wide variety of electrode geometries available. Each style has characteristic performance in heat distribution and final weld nugget geometry.

The weld joint chosen for the simulation is based on an Auto-Steel Partnership (A/SP) state-of-the-art B-pillar to rocker joint using 1.6 mm GI DP780 to 1.6 mm GI DP780. The A/SP has released a projected steel usage table and the B-pillar reinforcement joint was chosen for this project. Using the recommended 'state-of-the-art' material called for in this table, the objective of this work is to show which electrode geometries would yield the most robust welding procedures and best quality welds.

The steel was supplied from General Motors, the electrodes by Huys Industries Ltd., and the confirmatory welds, and related micrographic analyses, were performed at the University of Waterloo. The tool chosen to simulate the welds was Version 6.6 of

SORPAS® resistance welding software. This software allows for the user to understand and track nugget formation and overall weldability. At the same time, simulations can evaluate the thermal properties of the weld and track differences between the geometries during the weld.

### EXPERIMENTAL PROCEDURE

Four types of electrodes have been chosen to evaluate on the A/SP recommended joint configuration (Figure 1). All electrodes were RWMA Class 2-2 Cu-Cr-Zr material. These electrodes were compared based on weld current ranges or windows and nugget shape and size. The steel used according to A/SP for the B-pillar reinforcement joint will be 1.6 mm DP780 steel [Ref. 2]. Simulation software was used to generate weld current windows for each of the electrode geometries using the same weld schedule. The maximum and minimum nugget size predicted for each electrode geometry was then tested on laboratory coupons to confirm the findings of the simulation.

Geometry	Weld Face Diameter	Outer Diameter	Notes
FB-25 (B-nose)	4.8 mm	16 mm	8 mm dome radius
FB-25 (ISO F-nose)	6 mm	16 mm	8 mm dome radius
FE-25 (E-nose)	6 mm	16 mm	45° Truncation angle
ParaCap(TM)	6 mm	16 mm	Parabolic profile

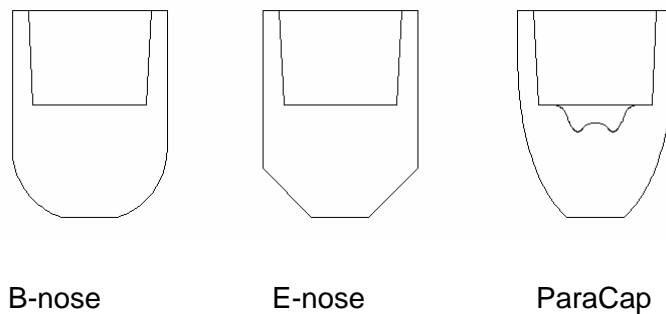


**Figure 1: Electrode Geometry Specifications**

#### Simulation Parameters

All simulations were carried out using FEA software SORPAS® Enterprise Edition 6.6 from Swantec Software and Engineering ApS [Ref. 3]. The typical simulation mesh is shown in Figure 2. Welding electrodes and work sheet configurations were entered into the simulation using a 2D co-ordinate mapping system to create objects. A materials database is then used to assign the object material properties as shown in Figure 3.

Once the objects have been created, the machine tools are specified to apply the weld force and current. A mesh of nodes is applied to the 2D image. Given the configuration used for the simulation it is required to have a minimum of 1000 nodes. The weld force and current can be characterized to match existing welding machines and controllers. At this stage, all welding parameters can be specified in the simulation. Finally, the simulation parameters can be adjusted to change simulation speed and accuracy. Automatic optimizations can also be setup to iterate simulations to find a specific weld nugget size or current range for weld lobe studies. Simulation parameters used in this study are shown in Table 1. All simulations for the various types of electrode geometries were setup identically except for the actual electrode geometry.

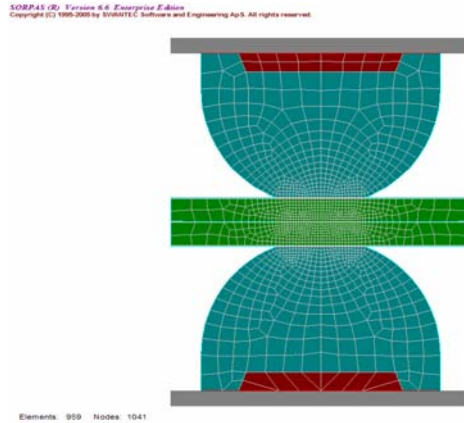


**Figure 2: Resistance Spot Welding Configuration for Simulation**

Property	20,000	50,000	100,000	150,000	200,000
HAZ T <sub>1</sub> [°C]	750,000				
HAZ T <sub>2</sub> [°C]	750,000				
HAZ T <sub>3</sub> [°C]	750,000				
HAZ T <sub>4</sub> [°C]	750,000				
HAZ T <sub>5</sub> [°C]	750,000				
HAZ T <sub>6</sub> [°C]	750,000				
HAZ T <sub>7</sub> [°C]	750,000				
HAZ T <sub>8</sub> [°C]	750,000				
HAZ T <sub>9</sub> [°C]	750,000				
HAZ T <sub>10</sub> [°C]	750,000				
HAZ T <sub>11</sub> [°C]	750,000				
HAZ T <sub>12</sub> [°C]	750,000				
HAZ T <sub>13</sub> [°C]	750,000				
HAZ T <sub>14</sub> [°C]	750,000				
HAZ T <sub>15</sub> [°C]	750,000				
HAZ T <sub>16</sub> [°C]	750,000				
HAZ T <sub>17</sub> [°C]	750,000				
HAZ T <sub>18</sub> [°C]	750,000				
HAZ T <sub>19</sub> [°C]	750,000				
HAZ T <sub>20</sub> [°C]	750,000				
HAZ T <sub>21</sub> [°C]	750,000				
HAZ T <sub>22</sub> [°C]	750,000				
HAZ T <sub>23</sub> [°C]	750,000				
HAZ T <sub>24</sub> [°C]	750,000				
HAZ T <sub>25</sub> [°C]	750,000				
HAZ T <sub>26</sub> [°C]	750,000				
HAZ T <sub>27</sub> [°C]	750,000				
HAZ T <sub>28</sub> [°C]	750,000				
HAZ T <sub>29</sub> [°C]	750,000				
HAZ T <sub>30</sub> [°C]	750,000				
HAZ T <sub>31</sub> [°C]	750,000				
HAZ T <sub>32</sub> [°C]	750,000				
HAZ T <sub>33</sub> [°C]	750,000				
HAZ T <sub>34</sub> [°C]	750,000				
HAZ T <sub>35</sub> [°C]	750,000				
HAZ T <sub>36</sub> [°C]	750,000				
HAZ T <sub>37</sub> [°C]	750,000				
HAZ T <sub>38</sub> [°C]	750,000				
HAZ T <sub>39</sub> [°C]	750,000				
HAZ T <sub>40</sub> [°C]	750,000				
HAZ T <sub>41</sub> [°C]	750,000				
HAZ T <sub>42</sub> [°C]	750,000				
HAZ T <sub>43</sub> [°C]	750,000				
HAZ T <sub>44</sub> [°C]	750,000				
HAZ T <sub>45</sub> [°C]	750,000				
HAZ T <sub>46</sub> [°C]	750,000				
HAZ T <sub>47</sub> [°C]	750,000				
HAZ T <sub>48</sub> [°C]	750,000				
HAZ T <sub>49</sub> [°C]	750,000				
HAZ T <sub>50</sub> [°C]	750,000				
HAZ T <sub>51</sub> [°C]	750,000				
HAZ T <sub>52</sub> [°C]	750,000				
HAZ T <sub>53</sub> [°C]	750,000				
HAZ T <sub>54</sub> [°C]	750,000				
HAZ T <sub>55</sub> [°C]	750,000				
HAZ T <sub>56</sub> [°C]	750,000				
HAZ T <sub>57</sub> [°C]	750,000				
HAZ T <sub>58</sub> [°C]	750,000				
HAZ T <sub>59</sub> [°C]	750,000				
HAZ T <sub>60</sub> [°C]	750,000				
HAZ T <sub>61</sub> [°C]	750,000				
HAZ T <sub>62</sub> [°C]	750,000				
HAZ T <sub>63</sub> [°C]	750,000				
HAZ T <sub>64</sub> [°C]	750,000				
HAZ T <sub>65</sub> [°C]	750,000				
HAZ T <sub>66</sub> [°C]	750,000				
HAZ T <sub>67</sub> [°C]	750,000				
HAZ T <sub>68</sub> [°C]	750,000				
HAZ T <sub>69</sub> [°C]	750,000				
HAZ T <sub>70</sub> [°C]	750,000				
HAZ T <sub>71</sub> [°C]	750,000				
HAZ T <sub>72</sub> [°C]	750,000				
HAZ T <sub>73</sub> [°C]	750,000				
HAZ T <sub>74</sub> [°C]	750,000				
HAZ T <sub>75</sub> [°C]	750,000				
HAZ T <sub>76</sub> [°C]	750,000				
HAZ T <sub>77</sub> [°C]	750,000				
HAZ T <sub>78</sub> [°C]	750,000				
HAZ T <sub>79</sub> [°C]	750,000				
HAZ T <sub>80</sub> [°C]	750,000				
HAZ T <sub>81</sub> [°C]	750,000				
HAZ T <sub>82</sub> [°C]	750,000				
HAZ T <sub>83</sub> [°C]	750,000				
HAZ T <sub>84</sub> [°C]	750,000				
HAZ T <sub>85</sub> [°C]	750,000				
HAZ T <sub>86</sub> [°C]	750,000				
HAZ T <sub>87</sub> [°C]	750,000				
HAZ T <sub>88</sub> [°C]	750,000				
HAZ T <sub>89</sub> [°C]	750,000				
HAZ T <sub>90</sub> [°C]	750,000				
HAZ T <sub>91</sub> [°C]	750,000				
HAZ T <sub>92</sub> [°C]	750,000				
HAZ T <sub>93</sub> [°C]	750,000				
HAZ T <sub>94</sub> [°C]	750,000				
HAZ T <sub>95</sub> [°C]	750,000				
HAZ T <sub>96</sub> [°C]	750,000				
HAZ T <sub>97</sub> [°C]	750,000				
HAZ T <sub>98</sub> [°C]	750,000				
HAZ T <sub>99</sub> [°C]	750,000				
HAZ T <sub>100</sub> [°C]	750,000				

**Figure 3: Materials Property Database in SORPAS®**

Replicating the electrode geometries with cooling water in the simulations was done using the exact geometry dimensions. Cooling water was set at 9°C to simulate the laboratory cooling water temperature. Welding windows were established using the A/SP recommended RSW parameter schedules for AHSS (Table 2). Minimum and maximum weld nugget sizes were outlined by American Welding Society (AWS) welding standards given in Table 3.

**Table 1: Simulation parameters for SORPAS®**

Simulation Parameters				
	Squeeze	Weld	Hold	
Time Step Increment	0.1	0.05	0.1	(ms)
Save Data Per	10	5	10	steps
Convergence Control				
	Convergence Accuracy			
Electrical Model	1.00E-05			
Thermal Model	1.00E-05			
Mechanical Model	1.00E-05			
Dynamic Contact Between Materials				
	Sliding			
Heat Loss to Surroundings				
Air Temperature	20			°C
Heat Transfer Rate	300			(W/m2K)

**Table 2: Welding Schedule Guidelines Courtesy of A/SP**

**Coated-to-Coated Faying Surface Conditions**

GMT Range (mm)	Weld Force	Weld Time	Cool Time	Number of Pulses	Weld Sequence (Cycles)	Hold Time (Cycles)	Electrode Size
1.45 - 1.64	950	21	1	3	7-1-7-1-7	5	2

**Table 3: Weld nugget size requirements**

Governing Metal Thickness (mm)	Minimum Weld Size (Note 1)	Weld Size Upper Limit (Note 2)	DCX Weldability DoE High Value
1.60 - 1.89	5.5	6.5	7.3

**Note 1** - Minimum weld sizes (MWS) are based on AWS D8.1M, Specification for Automotive Weld Quality - Resistance Spot Welding.

**Note 2** - Weld Size Upper Limit is based on AWS D8.1M minimum size plus 1.0mm.

The minimum and maximum weld nugget sizes were entered into the simulation software to find the proper weld current to achieve the target weld size. Weld force and time were held constant to conform to A/SP weld schedule guidelines. After the simulation provided the weld current necessary to form the upper and lower bounds of the weld window, the remainder of the current window was simulated in 200 A increments to track the growth of the nuggets from the minimum to maximum limits.

Weld width and penetration was monitored and was expected to change with various electrode geometries due to the differences in power density and cooling rates. [Ref. 4]

### **Laboratory Testing**

All lab testing was conducted on a 250kVA single phase AC pedestal welder. The upper and lower bounds for weld nugget size were tested using weld currents given by simulation. Each pair of electrodes was conditioned at 75% of the weld current for 50 welds before coupon welding was performed. Welds were made on peel coupons 50 mm x 140 mm. Welds were then cross sectioned to inspect the microstructure of the weld and confirm the accuracy of the simulation. The weld nugget geometry was analyzed by optical microscopy and compared to the results of the simulations.

## **RESULTS AND DISCUSSION**

### **Simulation Results**

#### **Weld Current Window**

Specific optimization of weld current to achieve a target weld size was performed for each electrode design. Predicted weld sizes, required weld current and maximum electrode temperature are given in Table 4. Using the weld current given in the table as the upper and lower bound of the weld current window, the entire weld window was then simulated in 200 A increments to yield one nugget size vs. weld current plot per electrode type as generated by the simulation software. These plots are given in Figure 4(a-d).

**Table 4: Predicted weld sizes, required weld current and maximum electrode temperature**

Electrode Type	FB-25 4.8 mm		FB-25 6 mm		FE-25 6 mm		ParaCap™ 6 mm	
Target Weld D (mm)	5.5	6.5	5.5	6.5	5.5	6.5	5.5	6.5
Predicted Weld D (mm)	5.44	6.5	5.5	6.5	5.4	6.45	5.5	6.5
Weld I Output (A)	6624	7993	7589	8811	7572	8780	7599	9130
Current Range (A)	1369		1222		1208		<b>1531</b>	
Max Electrode T (°C)	322	<b>458</b>	287	372	294	387	314	447

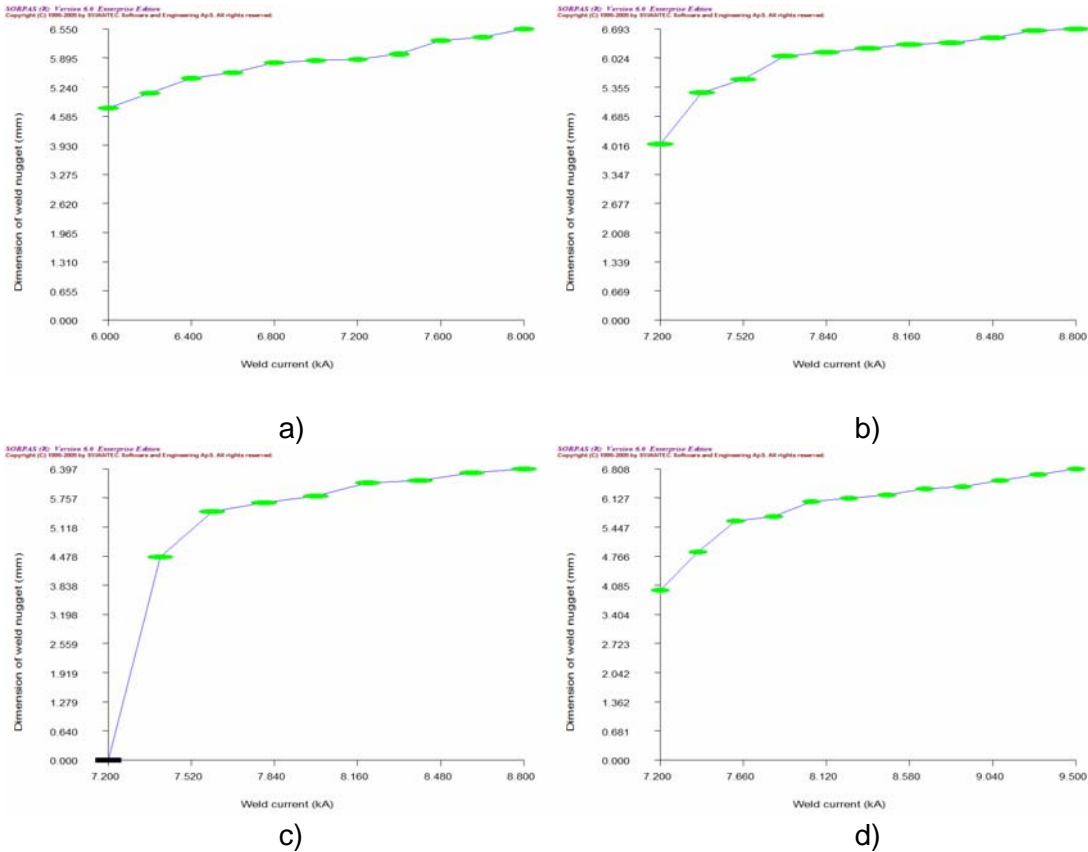


**Figure 4:** Current window for electrode geometries; a) FB-25 4.8 mm weld face; b) FB-25 6 mm weld face; c) FE-25 6 mm weld face; d) ParaCap™ 6 mm weld face

Of the geometries tested, the FB-25 with 4.8 mm face diameter yielded the lowest required current with a minimum weld current of 6624 A and 7993 A maximum. Peak temperature in the electrode was predicted to be 458°C. This was attributed to the reduced weld face area which increased the current density and the rate of heating of the steel. The usable weld current window was 1369 A which was very good compared to some of the other electrodes however due to the high current and heat density, expulsion and deformation was more severe.

The FB-25 electrode with the 6 mm weld face yielded a smaller weld current window of only 1222 A. The electrode peak temperature of 372°C was much lower than that of the 4.8mm weld face electrode with a minimum weld current of 7589 A and maximum of 8811 A. The increased contact area of the electrode resulted in a decreased current density requiring higher currents to achieve the target weld size.

The FE-25 truncated electrode had a predicted weld current window of 1208 A, the smallest of the group. The simulation also returned optimized weld nugget sizes slightly lower than the targets of 5.5 and 6.5 mm. Electrode peak temperatures were moderate yet higher than the B-nose 6mm face electrodes at 387°C. This suggests that the extraction of heat through the electrode was less thereby allowing more heat to be

retained in the steel yielding larger nuggets. The nominal current for a 6.5 mm nugget was predicted to be 8780 A, while the minimum required current was 7572 A.

The ParaCap™ electrode geometry displayed the greatest weld current window of 1531 A. According to simulations, this is the most robust electrode geometry for this steel stack-up configuration. Simulations were able to generate weld nuggets of exactly 5.5 and 6.5 mm as targeted with 7599 A and 9130 A respectively. Peak temperature of the electrodes during welding was 447°C, higher than both the other 6 mm weld face diameter geometries. Due to the higher current allowed within the required weld sizes, the added heat is expected.

Differences in electrode weld face contact area have been known to change the current density and thus the characteristics of the weld nugget. These simulations have shown that SORPAS® is able to predict changes to the nugget character based upon the overall geometry of the electrodes.

### Weld Size and Penetration

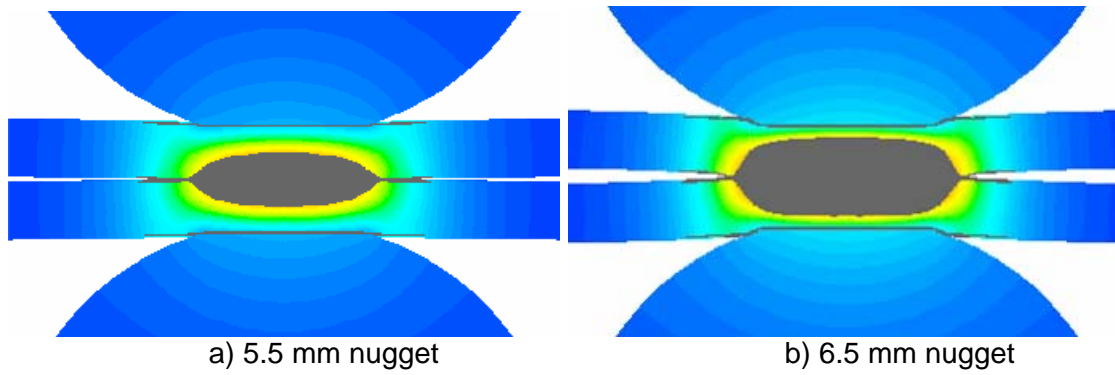
Table 5 shows numerically the predicted weld penetration of each of the electrodes at the 5.5 mm nugget and 6.5 mm nugget stages. The FB-25 4.8 mm weld face electrode clearly has the largest penetration with close to 50% of the sheet thickness for the 5.5 mm nugget condition. The 6.5 mm nugget condition is up to 70% penetration. Figure 5 shows the predicted weld for the FB-25 with 4.8 mm weld face at 5.5 mm and 6.5 mm nugget sizes. The shapes of the nuggets at both ends of the lobe are slightly rectangular with penetration at least 50% of the sheet. Sheet deformation is present for both conditions.

Figure 6 displays the predicted weld for the FB-25 electrode with 6 mm weld face. Predicted nugget shape at the 5.5 mm nugget point was rather narrow with only 19% penetration into the base material. The 6.5 mm nugget was much better with an increase in penetration up to approximately 54%. No sheet deformation was detected for either of the welds.

**Table 5: Predicted Weld Penetrations (1.6mm Sheet thickness)**

Electrode	Weld Penetration (mm)		Weld Penetration (%)	
	5.5 mm Nugget	6.5 mm Nugget	5.5 mm Nugget	6.5 mm Nugget
<b>FB-25 4.8 mm Face</b>	0.770	1.120	0.48	0.70
<b>FB-25 6 mm Face</b>	0.297	0.870	0.19	0.54
<b>FE-25 6 mm Face</b>	0.196	0.701	0.12	0.44
<b>ParaCap(TM) 6 mm Face</b>	0.325	1.020	0.20	0.64





**Figure 5: Predicted weld shape for FB-25 4.8 mm Electrodes**

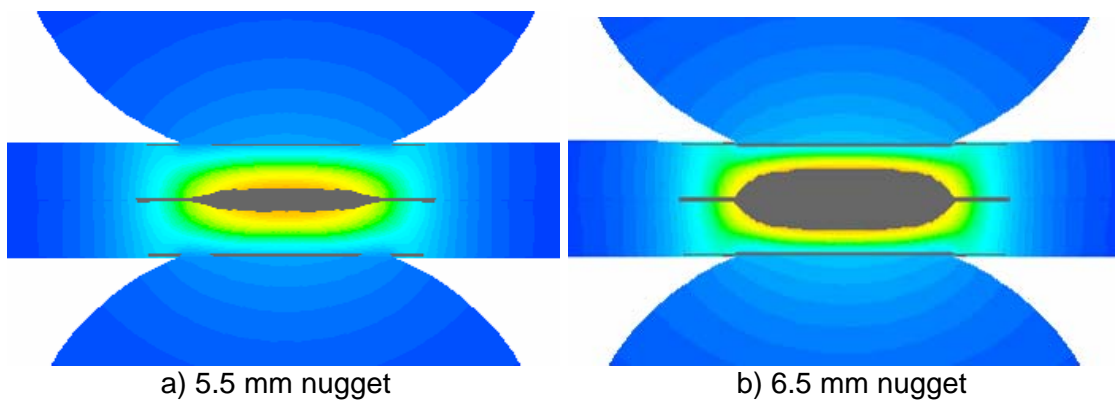


**Figure 6: Predicted weld shape for FB-25 6 mm Electrodes**

Figure 7 shows the simulation results for the FE-25 6 mm weld face electrodes. The nuggets are very narrow with only 12% and 44% for the 5.5 mm and 6.5 mm nuggets respectively. Nugget shapes are very sharp at the edges and no deformation is detected. This electrode was predicted to have the smallest weld current range, as well as the narrowest nuggets.

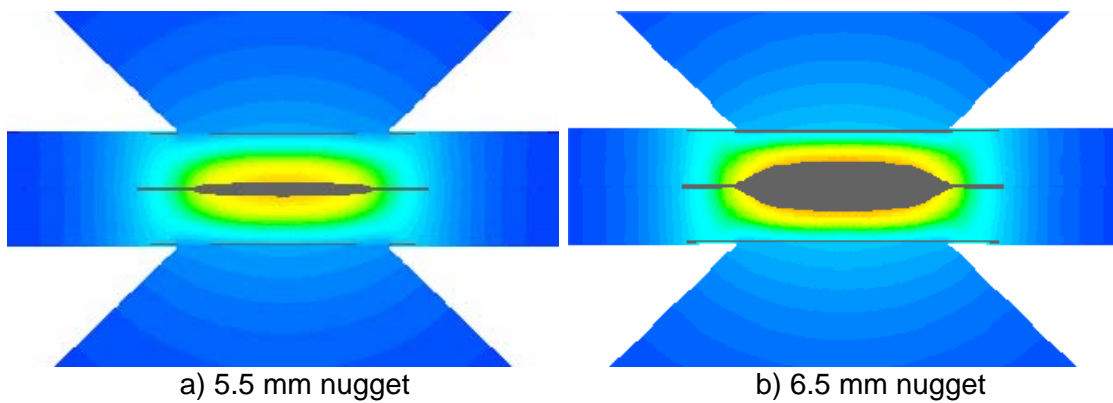


**Figure 7: Predicted weld shape for FE-25 6 mm Electrodes**

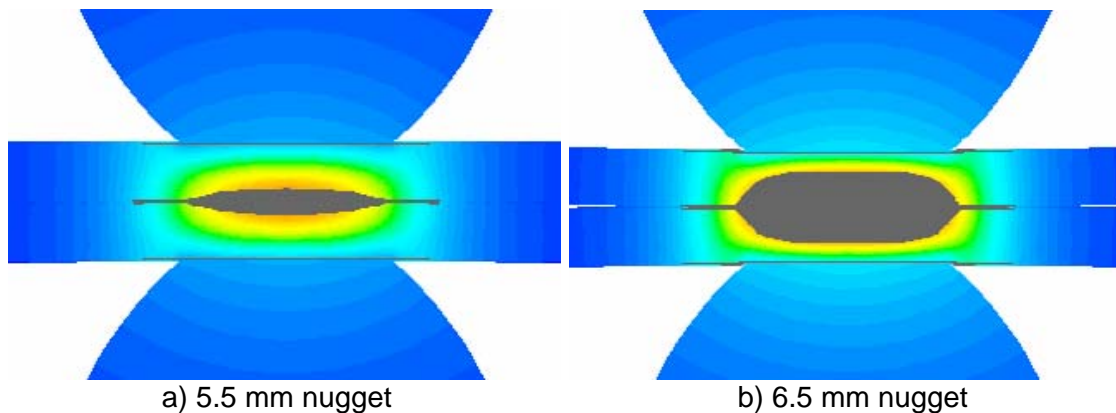


**Figure 8: Predicted weld shape for ParaCap™ 6 mm Electrodes**

Figure 8 displays the results for the ParaCap™ 6 mm weld face electrodes. With weld penetrations at 20% and 64% for 5.5 mm and 6.5 mm nuggets, these electrodes have been predicted to have the best penetration and weld current range of the 6mm weld faced electrodes. The weld shape for the 6.5 mm nugget was slightly more rectangular than the FE-25 electrodes however not as much as the FB-25 electrodes. There is also very slight weld deformation detected in the 6.5 mm nugget condition.

### **Laboratory Verification**

Side by side comparisons of the varying effects of different electrode geometries are shown in Figure 9. Comparing the metallographic and simulation results a correlation can be made. However, as the predicted nugget diameters were measured at the nugget diameter relative to the melted region at the interface of the two materials, vertical growth of the nugget or penetration was not set as a criteria. This resulted in predicted nugget diameters and weld schedule outputs which were slightly over predicted. This was more prevalent in the case of the 5.5 mm nugget condition. Such nugget shapes are indicative of a centerline fracture that has been noticed in DP600 Steels [Ref. 5]. The upper limit welds at 6.5 mm do not seem to have this issue of over-predictions to the same degree.

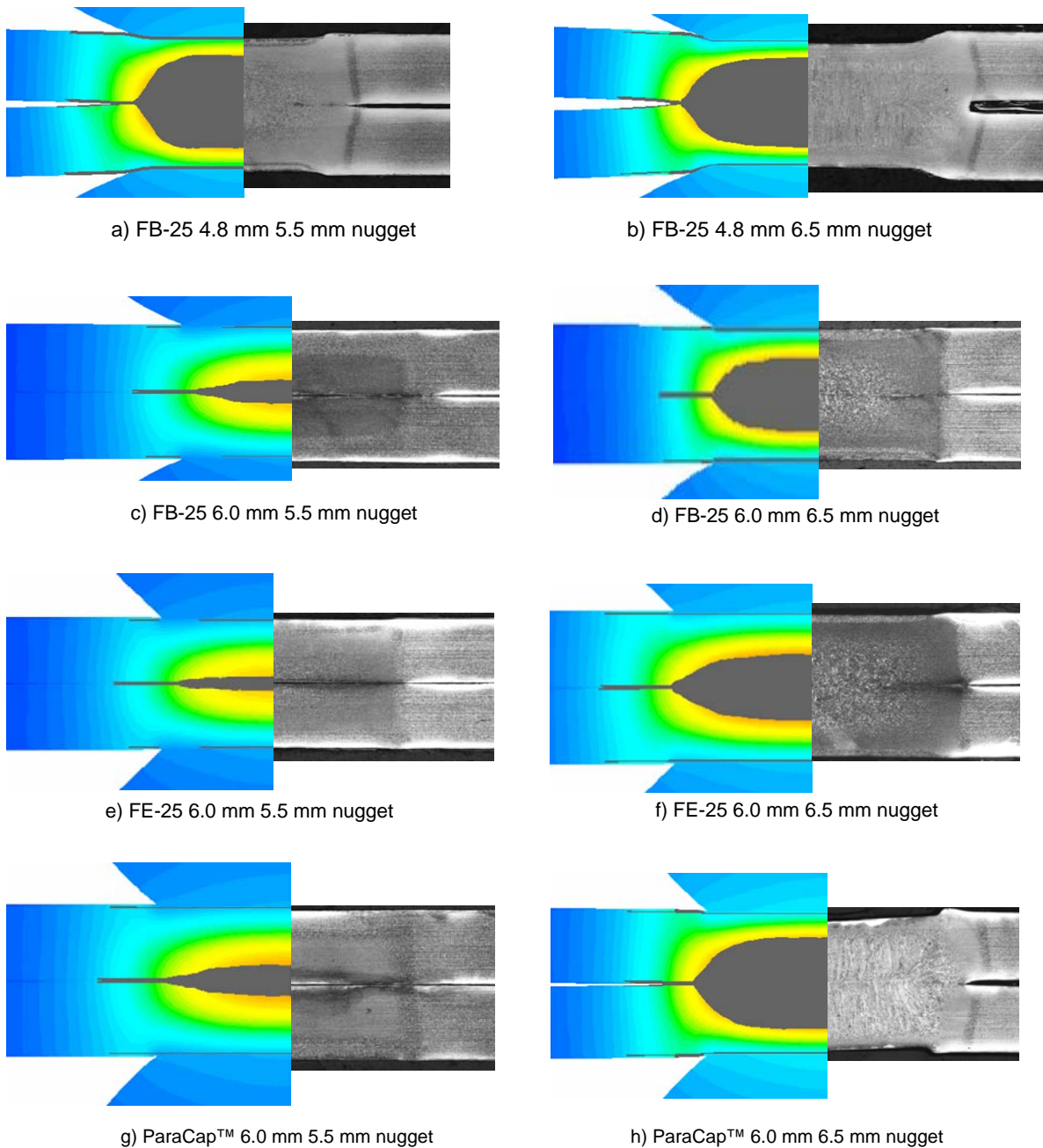


**Figure 9: Weld Cross-sections compared to simulation results.**

Overall the degree of deformation predicted was seen in the actual weld samples. Weld cross-sections for the FB-25 4.8 mm weld face and the ParaCap™ 6.5 mm weld show indentation and slight separation of the sheets adjacent to the nuggets. The differences in the weld nugget shape are also seen in the weld cross-sections. The sharpness of the FE-25 electrode at the 6.5 mm nugget condition can faintly be seen in contrast to the FB-25 electrodes with the rectangular nugget. Although further detailed lab studies are still required for improved verification, it is clear that the simulations were able to predict

the general behaviour of the different electrode geometries with respect to their relative differences in weld shape and weld schedule.

## CONCLUSION

Without a thorough understanding of how to weld the new Advanced High Strength Steels, their use and benefits within the automotive industry will be restricted. Finite element modeling of Advanced High Strength Steels for both weldability and process optimization is both possible and practicable. Finite element modeling presents a significant opportunity to reduce but not eliminate traditional laboratory experimentation for assessing material weldability.

Electrode geometry does affect the development and final shape of the weld nugget.

Through FEA modelling, it has been shown that the ParaCap™ electrode geometry with a 6mm weld face yielded the largest weld current window when welding 1.6 mm DP780 steel for the conditions studied.

Electrode temperature and deformation was found to be more pronounced when using the FB-25 4.8 mm electrode. The FB-25 (ISO F-style) electrode with 6 mm contact face while able to reduce the heating of the electrode and indentation of the steel, however did not provide a current range as great as the ParaCap™. The FE-25 6 mm showed a current range similar to the FB-25 6 mm however nugget penetration was reduced.

## REFERENCES

- (1) Biro E., Lee A, Welded Properties of Various DP600 Chemistries *SMWC* 2004
- (2) A/SP AHSS Applications Recommendations, February 8, 2005
- (3) Swantec Software and Engineering ApS, Denmark, [www.swantec.com](http://www.swantec.com)
- (4) Parker, J. D., Williams, N. T., Holliday, R. J., "Mechanisms of electrode degradation when spot welding coated steels", *Science and Technology of Welding and Joining*, 1998, Vol. 3, No. 2, pp. 65-74
- (5) Marya M. , Gayden, X.Q. 2006, Development of requirements for resistance spot welding Dual-Phase (DP600) steels part 1 - The causes of interfacial fracture. *Welding Journal (Miami, Fla)*, v 84, n 11